L. York, *ibid.*, **10**, 840 (1971); H. B. Gray, *Adv. Chem. Ser.*, No. **100**, 365 (1971); J. W. Dawson et al., *Biochemistry*, **11**, 461 (1972).
(3) J. San Filippo, Jr., R. L. Grayson, and H. J. Sniadoch, *Inorg. Chem.*, **15**, 269 (1976).
(4) (a) W. Kiefer and H. J. Bernstein, *Appl. Spectrosc.*, **25**, 500 (1971); (b) *ibid.*, **25**, 609 (1971).
(5) R. Colton and G. G. Rose, *Aust. J. Chem.*, **21**, 883 (1968).
(6) (a) J. L. Woodhead and J. H. Fletcher, A.E.R.E. Report, 4123 (Hartwell), England, 1962; (b) I. P. Alimarin, V. I. Shlenskaya, and Z. A. Kuratashvili, *Russ. J. Inorg. Chem.* (*Engl. Transl.*), **18**, 250 (1973).
(7) R. E. Hester, "Raman Spectroscopy", H. A. Symanski, Ed., Plenum Press, New York, N.Y., 1967, Chapter 4.
(8) The molecular symmetry of the $M_2OX_{10}^{4-}$ ion is D_{4h}. In this point group the totally symmetric vibrations (A_{1g}) have scattering tensors with diagonal elements only: α'_{xx}, α'_{yy}, α'_{zz}. Under such circumstances the depolarization ratio can be shown[7] to have the form

$$\rho_1 = {}^1/_3 \frac{(\alpha'_{xx})^2 + (\alpha'_{yy})^2 + (\alpha'_{zz})^2 - \alpha'_{xx}\alpha_{yy} - \alpha'_{xx}\alpha'_{zz} - \alpha'_{yy}\alpha'_{zz}}{(\alpha'_{xx})^2 + (\alpha'_{yy})^2 + (\alpha'_{zz})^2 + {}^2/_3\alpha'_{xx}\alpha'_{yy} + {}^2/_3\alpha'_{xx}\alpha'_{zz} + {}^2/_3\alpha'_{yy}\alpha'_{zz}}$$

When one element is dominant, this reduces to $\rho_1 \simeq {}^1/_3$.
(9) R. S. Chao, R. K. Khanna, and E. R. Lippincott, *J. Raman Spectrosc.*, **3**, 121 (1975).
(10) It has been suggested[9] that when discussing solid-state resonance Raman data, it may actually be preferable to employ the maximum in the excitation profile determined from solid-state Raman intensity data as the effective electronic frequency, ν_e, rather than the value traditionally obtained from the solution UV-vis spectrum.
(11) Following the completion of our earlier study (ref 3) an investigation detailing the crystal structure of $K_4W_2OCl_{10}$ and its isostructural relationship to $K_4Re_2OCl_{10}$, $K_4Ru_2OCl_{10}$, and $Cs_4Os_2OCl_{10}$ appeared: T. Glowiak, M. Sabat, and B. Jezowska-Trzebiatowska, *Acta Crystallogr., Sect. B*, **31**, 1783 (1975).
(12) E. König, *Inorg. Chem.*, **8**, 1278 (1969).
(13) M. E. Lines, A. P. Ginsberg, and F. J. Di Salvo, *J. Chem. Phys.*, **61**, 2095 (1974).
(14) A. P. Ginsberg, *Inorg. Chim. Acta, Rev.*, **5**, 45 (1971).
(15) At 110 K the g value for solid $K_4W_2OCl_{10}$ as determined by ESR is 1.778. A similar value (g = 1.76 at 25 °C) was previously reported by R. Colton and G. G. Rose, *Aust. J. Chem.*, **21**, 883 (1968).
(16) B. Jezowska-Trzebiatowska, J. Hanuza, and W. Wojciechowski, *J. Inorg. Nucl. Chem.*, **28**, 2701 (1966).
(17) These observations compare favorably with the solution absorption spectrum of $(NH_4)_4[Os_2OCl_{10}]$ reported in ref 16. In addition, these authors also report the appearance of a broad band in the near-IR region, centered at 1050 nm (ϵ 240).
(18) The reflectance spectrum of $(NH_4)_4Os_2OCl_{10}$ was too diffuse and ill-defined to permit a meaningful comparison to the solution spectrum.
(19) J. San Filippo, Jr., *Inorg. Chem.*, **11**, 3140 (1972).
(20) J. D. Dunitz and L. E. Orgel, *J. Chem. Soc.*, 2594 (1953).
(21) See also W. Klemm and K. H. Raddatz, *Z. Anorg. Allg. Chem.*, **250**, 207 (1942); B. N. Figgis and J. Lewis, *Prog. Inorg. Chem.*, **6**, 148 (1964).
(22) Transitions involving electrons from the σ framework are likely to occur at much higher energies than the resonating electronic transition observed in the present study and for this reason are not considered in the present discussion.
(23) This statement follows from a consideration of the magnitude of the transition dipole moment, μ, in the approximate expansion of the relevant MO in terms of atomic orbitals localized on M_1, M_2, and O.

$$\mu_{e_g \rightarrow e_u{}^a} = \langle d_{xz}(M_1)\mu d_{xz}(M_1)\rangle - \langle d_{xz}(M_2)\mu d_{xz}(M_2)\rangle - \langle d_{xz}(M_2)\mu \underset{y}{p_x}(O)\rangle + \langle d_{xz}(M_2)\mu \underset{y}{p_x}(O)\rangle = -2\langle d_{xz}(M_2)\mu d_{xz}(M_2)\rangle$$

which reduces to $\mu_{e_g \rightarrow e_u{}^a} = -2\mathbf{R}_{M\text{-}O}$, where $\mathbf{R}_{M\text{-}O}$ is the length of the metal oxygen bond. However, at the same level of approximation

$$\mu_{b_{2g}} \rightarrow e_u{}^a = \langle d_{xy}(M_1)\mu \underset{yz}{d_{xz}}(M_1)\rangle + \langle d_{xy}(M_2)\mu \underset{yz}{d_{xz}}(M_2)\rangle - \langle d_{xy}(M_1)\mu \underset{y}{p_x}(O)\rangle - \langle d_{xy}(M_2)\mu \underset{y}{p_x}(O)\rangle = 0$$

We conclude, therefore, that only the $e_g \rightarrow e_u{}^a$ transition can be expected to have an appreciable intensity. Moreover, it can be shown by local symmetry arguments that this transition will have z polarization.
(24) R. Shandles, E. O. Schlemper, and R. K. Murmann, *Inorg. Chem.*, **10**, 2785 (1971).
(25) D. L. Toppen and R. K. Murmann, *Inorg. Nucl. Chem. Lett.*, **6**, 139 (1970).
(26) S. J. Lippard, H. J. Schugar, and C. Walling, *Inorg. Chem.*, **6**, 1825 (1967).
(27) H. J. Schugar, G. R. Rossman, C. G. Barraclough, and H. B. Gray, *J. Am. Chem. Soc.*, **94**, 2683 (1972).

Contribution from the Materials and Molecular Research Division, Lawrence Berkeley Laboratory, Berkeley, California 94720, and the Chemistry Division, Atomic Energy Research Establishment, Harwell, England

Spectral Properties of $(Et_4N)_2UI_6$ and $(Et_4N)_2UF_6$

W. WAGNER,[1a] N. EDELSTEIN,*[1a] B. WHITTAKER,[1b] and D. BROWN*[1b]

Received November 23, 1976 AIC60845T

The optical spectra of $(NEt_4)_2UI_6$ and $(NEt_4)_2UF_6$ are presented and analyzed. With these data the electrostatic, spin–orbit, and crystalline field parameters have been obtained for the series of octahedral compounds UX_6^{2-} (X = F, Cl, Br, I). The Slater parameter F^2 diminishes approximately 20% as the halide ion changes from F^- to I^-. The crystalline (or ligand) field parameters for comparable PaX_6^{2-} and UX_6^{2-} compounds vary markedly.

Introduction

The preparation and spectral properties of octahedral compounds of the type $(NEt_4)_2PaX_6$ (X = F, Cl, Br, I) have recently been investigated.[2,3] The trends in the ligand field parameters θ and Δ for these $5f^1$ complexes were explained qualitatively in terms of molecular orbital theory by large variations in σ bonding dominating the total ligand field splitting and changing markedly as the halide ion varied. This same trend was also found for salts of the hexahalogenouranates (V). As part of the above program the corresponding $(NEt_4)_2UX_6$ (X = F, Cl, Br, I) salts were prepared and their optical spectra obtained at 77 K.[2b,3] The most thorough analyses of the octahedral UX_6^{2-} spectra (X = Cl, Br) have been given by Satten and co-workers from data obtained at 4 K on U^{4+} diluted in single crystals.[4-6] We report in this paper the analyses of the spectra of $(NEt_4)_2UX_6$ (X = I, F) and compare the trends in the parameters obtained for the U^{4+} series ($5f^2$) as the halide ion is varied, with the corresponding parameters in the $5f^1$ series.

Experimental Section and Calculations

The preparation of $(NEt_4)_2UI_6$ and $(NEt_4)_2UF_6$ and the recording of their spectra at room temperature and 77 K have been described previously.[2,3,7]

Calculated energies were obtained by the simultaneous diagonalization of the combined electrostatic, spin–orbit, and crystalline field matrices which were constructed by the tensor operator methods described by Judd[8] and Wybourne.[9] These matrices were factored by the crystal quantum number, μ, into a 25 × 25 matrix (μ = 0, Γ_1 and Γ_2 states), a 24 × 24 matrix (μ = 2, Γ_3 and Γ_4 states), and two 21 × 21 matrices (μ = 1, a doubly degenerate Γ_5 state). Matrices of these ranks can be easily diagonalized by existing computer programs so no further factoring was necessary. Experimental energies were compared with calculated energies and the parameters of the

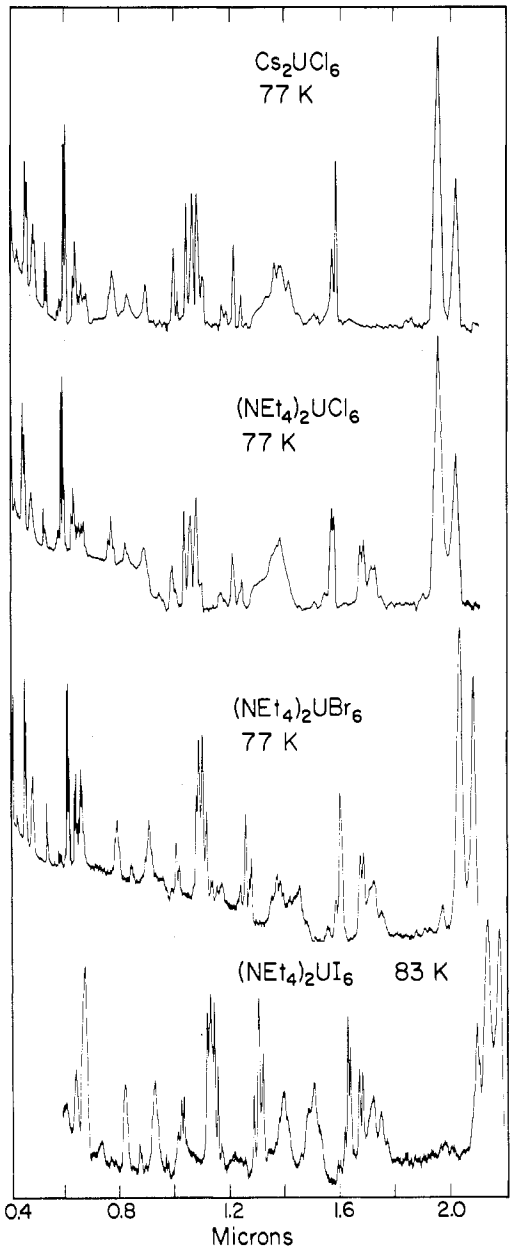

Figure 1. Spectra obtained for various UX_6^{2-} (X = Cl, Br, I) compounds at ~77 K. The lines at ~1.7 μ are from the NEt_4^+ cation.

above interactions were adjusted to provide the best fit. Our computer program was checked by reproducing the energy levels for Cs_2UBr_6 and Cs_2UCl_6 given by Satten et al.[4] using their parameters.

The crystal field Hamiltonian for octahedral symmetry was defined as

$$\mathcal{H}_c = B_0^4[C_0^{(4)} + (5/14)^{1/2}(C_{-4}^{(4)} + C_4^{(4)})] + B_0^6[C_0^{(6)} - (7/2)^{1/2}(C_{-4}^{(6)} + C_4^{(6)})]$$

following the nomenclature given by Wybourne.[9] For our calculations we set the ratios of $F^4/F^2 = 0.74$ and $F^6/F^2 = 0.55$.[10,11] These ratios were obtained from a review of the data available from spectra of free ions and trivalent 4f and 5f ions in the solid state and were found to be constant for a wide range of measurements.[12]

Results

Figure 1 shows the spectra obtained for $(NEt_4)_2UX_6$ (X = Cl, Br, I) and for Cs_2UCl_6. As can be seen immediately the general features of these spectra are very similar, the UI_6^{2-} spectrum showing shifts to lower energies when compared to the UBr_6^{2-} and UCl_6^{2-} spectra. The situation for $(NEt_4)_2UF_6$ is quite different as shown in Figure 2. This spectrum shows almost no similarity to the other UX_6^{2-} spectra and the peaks are strongly shifted to higher energies.

High-resolution optical spectra of UCl_6^{2-} and UBr_6^{2-} have been studied in great detail by Satten and co-workers.[4-6] These spectra are dominated by vibronic transitions which appear at regularly spaced intervals on either side of the pure electronic transitions. For O_h symmetry the pure electronic dipole transition within an l^n configuration is forbidden; however, vibrations of ungerade character break the inversion symmetry and are observed superimposed upon the pure electronic transition. In some instances the pure electronic transitions are not observed but are deduced from the vibronic assignments. Satten and co-workers have interpreted in this fashion the spectra of UCl_6^{2-} and UBr_6^{2-}. We make use of their assignments and similarly assign the UI_6^{2-} spectrum.

The vibrational frequencies for UBr_6^{2-} and UCl_6^{2-} have been studied extensively[4-6,13-15] and we estimate the corresponding values for UI_6^{2-} by use of the equation[3]

$$\nu_i(\mathrm{I}) = \left[\frac{M(\mathrm{Cl\ or\ Br})}{M(\mathrm{I})}\right]^{1/2} (\nu_i(\mathrm{Cl\ or\ Br})) \qquad (1)$$

where ν_i is the frequency of the halide atom–metal vibration and M is the mass of the halide atom, and the data reported by Brown et al.[16] The calculated values are given in Table I and compared with the available measurements.

From the estimated and measured vibrational frequencies and by comparison with other UX_6^{2-} (X = Cl, Br) spectra we assigned eight electronic levels as shown in Table II. The vibrational frequencies observed do not fit well with the values expected for ν_3 and ν_4. The discrepancies could be due to errors in choosing the centers of overlapping peaks and/or the possibility of other normal modes or combinations of normal modes falling in these ranges also. However, the assignments

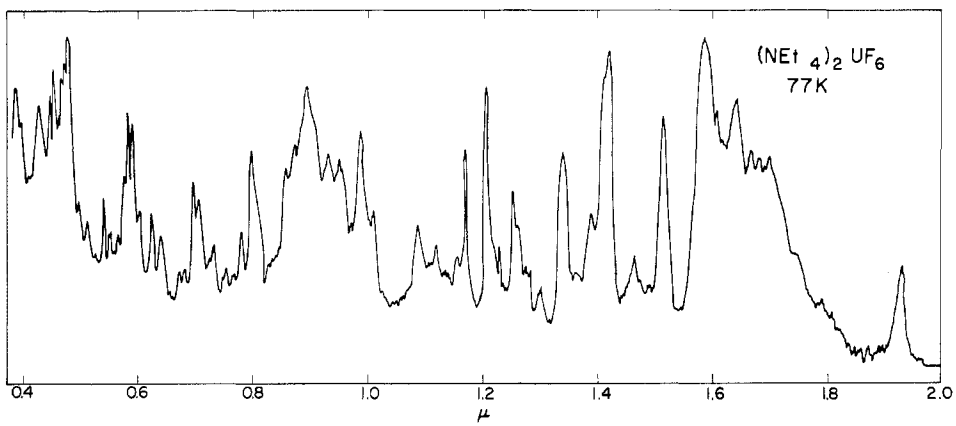

Figure 2. Spectrum of $(NEt_4)_2UF_6$ at 77 K. The lines at ~1.7 μ are from the NEt_4^+ cation.

Table I. Estimated Vibrational Frequencies (cm^{-1}) for $(Et_4N)_2UF_6$ and $(Et_4N)_2UI_6$

	UF_6^{2-}				UI_6^{2-}			
	Calcd		Obsd		Calcd		Obsd	
	UBr_6^{2-} [a]	UCl_6^{2-} [b]	PaF_6^{2-} [c]	UF_6^{2-} [c]	UBr_6^{2-} [a]	UCl_6^{2-} [b]	PaI_6^{2-} [d]	UI_6^{2-} [d]
ν_1	371	404			143	156		
ν_2	308				119			
ν_3	369	351	404	406	143	135	143	143
ν_4	168	155	148	155	65	60	60	60
ν_5	170	162			66	62		
ν_6	121	114			47	44		

[a] Reference 15. [b] References 5, 13. [c] Reference 2b. [d] Reference 3.

Table II. Observed Electronic and Vibronic Lines (cm^{-1}) and Assignments

$(NEt_4)UI_6$				$(NEt_4)_2UF_6$			
Vibronic lines	Vibrational freq	Electronic transition	Assignment	Vibronic lines	Vibrational freq	Electronic transition	Assignment
4596	−41			5 181	−457		
	0	4637	Γ_5	5 348	−290		
4680	+43				0	5638	Γ_5
4753	+116			6 094	+456		
4769	0	4769	Γ_3	6 006	+665		
				6 215	−456		
6112	−72			6 309	−362		
6143	−41				0	6671	Γ_3
6184	0	6184	Γ_4	7 032	+361		
6250	+66			7 087	+416		
6285	+101			7 342	+671		
6549	−91			6 605	−412		
6640	0	6640	Γ_5	6 821	−196		
6734	+94				0	7017	Γ_4
7092	−77			7 189	+184		
7169	0	7169	Γ_4	7 452	+435		
7262	+93			7 692	+675		
7570	−93			7 849	−441		
7663	0	7663	Γ_3	7 930	−360		
7782	+119				0	8290	Γ_4
				8 651	+361		
8643	−98			8 787	+497		
8741	0	8741	Γ_5	8 945	+655		
8842	+101						
				7 981	−596		
9606	−114			8 137	−440		
9671	−49			8 210	−367		
	0	9720	Γ_4		0	8577	Γ_5
9747	+27			8 945	+368		
9852	+132			9 225	+648		
				9 901	−661		
				10 111	−451		
					0	10562	Γ_5
				11 013	+451		
				11 274	+712		
				11 587	−448		
				11 655	−380		
					0	12035	Γ_4
				12 330	+295		
				12 484	+449		

were primarily made on the basis of the similarities with other UX_6^{2-} (X = Cl, Br) spectra.

By comparing the experimental energies with the calculated spectrum we were able to make three more assignments as shown in Table III. This table also shows the calculated and experimental energy levels. The parameters obtained by the "best fit" are given in Table IV. We also observed a small shift in the spectra of $(NEt_4)_2UX_6$ (X = Br, Cl) from that found by Satten et al. for the Cs_2UX_6 (X = Cl, Br). We assigned these spectra and obtained the "best fit" parameters

Table III. Calculated and Observed Electronic Transitions

$(Et_4N)_2UI_6$			$(Et_4N)_2UF_6$		
	Transition, cm^{-1}			Transition, cm^{-1}	
Γ	Exptl	Calcd	Γ	Exptl	Calcd
1	0	102	1	0	46
4		892	4		1 129
3		1 189	3		1 311
5		2 234	5		3 303
5	4 637	4 632	5	5 638	5 631
3	4 769	4 821	3	6 671	6 596
4	6 184	6 184	4	7 017	7 006
5	6 640	6 840	4	8 290	8 256
4	7 169	6 927	5	8 577	8 550
3	7 663	7 463	1	8 787	8 751
1		7 718	3	9 085	9 079
4		8 760	5		10 418
5	8 741	8 866	4	10 562	10 713
3		9 317	2		10 816
2		9 420	3		11 193
4	9 720	9 584	4	12 035	12 015
5		10 333	5	12 804	12 811
3	10 776	10 812	3	13 038	13 093
5		10 848	5	13 263	13 282
2	11 468	11 621	2		13 967
5	12 180	12 219	1		14 572
1		12 439	5	14 925	14 949
4		12 507	4		15 242
1		13 673	1	16 584	16 551
4		14 597	4	17 301	17 330
3		14 622	3	18 051	18 119
5		15 086	5		18 910
1		15 628	5		20 036
3		15 864	3		20 056
5		16 312	1		20 065
4		17 724	4		22 482
5		18 363	5		22 619
1		18 384	1		23 025
4		18 536	4		23 183
2		19 219	2		24 387
5		19 946	5		25 149
3		20 085	3		25 382
5		21 861	5		27 121
3		23 106	3		28 780
1		35 750	1		45 447

shown in Table IV and the energy levels given in Figure 3.

The interpretation of the spectrum of $(NEt_4)_2UF_6$ posed a more difficult problem. The vibrational frequencies expected were calculated by use of eq 1 and are given in Table I along with the reported values obtained from the vibronic spectrum of PaF_6^{2-} and IR measurements on UF_6^{2-}.[2b,17] The vibrational frequencies for UF_6^{2-} are much higher than for the other halides so they were well resolved in the spectrum. The most consistent vibrational frequency was observed at ~360 cm^{-1}. This value corresponds with that calculated for ν_3 (see Table I) but disagrees with the assignment obtained from the IR spectrum.[2] The energy levels for UF_6^{2-} were shifted strongly to higher energies but the same general ordering was expected as found for the other UX_6^{2-} complexes. On this basis the assignments given in Table II were made. For levels above

Table IV. Electrostatic, Spin-Orbit, and Crystalline Field Parameters (cm^{-1}) for UX_6^{2-} and PaX_6^{2-}

	UF_6^{2-} [a]	UCl_6^{2-} [a]	UBr_6^{2-} [a]	UI_6^{2-} [a]	UCl_6^{2-} [b]	UBr_6^{2-} [b]	PaF_6^{2-} [c]	$PaCl_6^{2-}$ [c]	$PaBr_6^{2-}$ [c]	PaI_6^{2-} [c]
F^2	49 699 ±465	43 170 ±2181	40 867 ±2739	38 188 ±2422	42 606	41 425				
ζ	1970 ±10	1774 ±35	1756 ±41	1724 ±39	1800	1792	1508	1523	1535	1542
B_0^4	10 067 ±113	7463 ±432	6946 ±609	6338 ±676	7211	6593	14 736	6666	5413	4191
B_0^6	22 ±72	992 ±258	999 ±252	941 ±289	1367	1195	1423	394	−68	−282
Δ_{rms} [d]	67	168	176	188						
Δ_{med} [e]	39	76	95	106						

[a] This work. [b] Reference 4. [c] Reference 3. [d] Root-mean-square deviation. [e] Mean energy deviation.

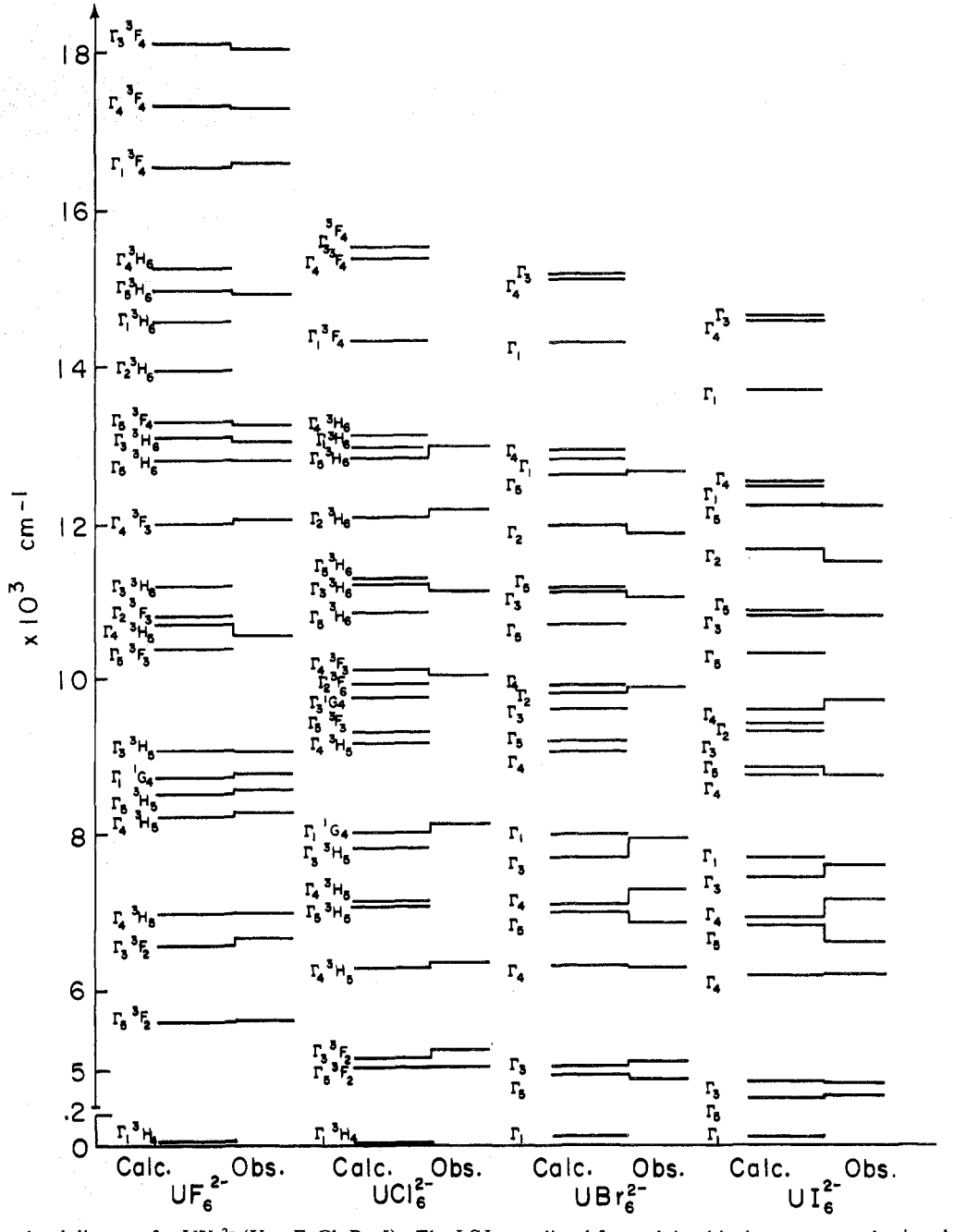

Figure 3. Energy level diagram for UX_6^{2-} (X = F, Cl, Br, I). The LSJ state listed for each level is the component having the largest value.

12000 cm^{-1} the assignments were determined by the proximity of the calculated and observed levels. The parameters are given in Table IV and the energy levels are shown in Figure 3.

It can be seen from Figure 3 that several pairs of energy levels for UF_6^{2-} are interchanged when compared to the energy levels of the other halide complexes. This change in order was necessary to obtain good agreement between the calculated

Table V. Ligand Field Parameters (cm^{-1}) for UX_6^{2-} and PaX_6^{2-}

	θ[a]		Δ[a]		ζ	
	M = Pa[b]	M = U	M = Pa[b]	M = U	M = Pa[b]	M = U
MF_6^{2-}	4502	2455	3074	3029	1508	1969 ± 10
MCl_6^{2-}	1873	2457	1634	1290	1523	1774 ± 35
MCl_6^{2-} [c]		2640		847		1800
MBr_6^{2-}	1268	2336	1707	1127	1535	1756 ± 41
MBr_6^{2-} [c]		2378		828		1792
MI_6^{2-}	832	2151	1546	999	1542	1724 ± 39

[a] Total ligand field splitting = $\Delta + \theta$. (See ref 2a for definitions.) [b] Reference 3. [c] Reference 5.

and observed levels. In one case this changeover can be directly traced from the spectra. The spectrum of $(NEt_4)_2UI_6$ shows well-resolved lines at 6640 cm^{-1} (Γ_5) and 7169 cm^{-1} (Γ_4). For the UBr_6^{2-} complex these two lines come closer and for UCl_6^{2-} we observe only a broad line with unresolved structure. Finally in $(NEt_4)_2UF_6$ we find again two well-resolved levels with the inverse order (8290 cm^{-1}, Γ_4; 8577 cm^{-1}, Γ_5).

Discussion

The electrostatic, spin–orbit, and crystalline field parameters obtained from our analyses and from Satten et al.[4] are tabulated in Table IV. One trend is immediately evident. All parameters except B_0^6 increase as the halide ion is changed from I^- to F^-. The change is most abrupt from Cl^- to F^- as expected from the spectra. The crystalline field parameters for the analogous PaX_6^{2-} and UX_6^{2-} compounds were expected to be similar, with the Pa parameters larger due to the greater magnitude of the radial expectation values $\langle r^n \rangle$. The effects due to the larger radial values for Pa^{4+} would be offset to a degree by the smaller ionic radius of U^{4+}. In fact, except for the fluoride complexes, the crystalline field parameters given in Table IV show none of the expected trends.

The difference between PaX_6^{2-} and UX_6^{2-} arises from the addition of a 5f electron so that in the $5f^2$ case we have the additional electrostatic parameters F^2, F^4, and F^6. Our calculations were performed with fixed ratios for F^4/F^2 and F^6/F^2 so we discuss only F^2. One of the surprising results of our analysis is the great change in F^2 as the halide ion is varied, of the order of 20%. In order to check this result we have also calculated the effect of fixed values for the configuration interaction parameters α, β, and γ (obtained from the results of the analysis of Np^{3+} diluted in $LaCl_3$[18]) and found no significant change in the fit of experimental and calculated levels nor in the empirical parameters.

We compare in Table V the values of Δ and θ,[1] the parameters obtained from ligand field theory, for the PaX_6^{2-} and UF_6^{2-} complexes. The value of Δ, the parameter which depends only on π bonding, is the same for the UF_6^{2-} and PaF_6^{2-} complexes; but although it is diminished for the other UX_6^{2-} complexes relative to the PaX_6^{2-} complexes, it is approximately constant. However, θ, which depends on both π and σ bonding, is relatively constant for the entire UX_6^{2-} series, in striking contrast to the PaX_6^{2-} which shows a substantial lowering as the halide ion is changed from F^- to I^-. The spin–orbit coupling constant ζ also changes more markedly for the UX_6^{2-} series than for the PaX_6^{2-} series.

Let us consider only the electrostatic and spin–orbit parameters. For the PaX_6^{2-} complexes the spin–orbit parameters are approximately equal for all three compounds while for the UX_6^{2-} complexes there is a significant decrease in this parameter between UF_6^{2-} and the other compounds. Qualitatively, we can attribute a reduction in the spin–orbit parameter to covalency effects, which would then appear to be significant in the chloride, bromide, and iodide complexes and in PaF_6^{2-}, but not in the UF_6^{2-} complex. Again, the difference between the PaF_6^{2-} and UF_6^{2-} complex may be attributed to the greater

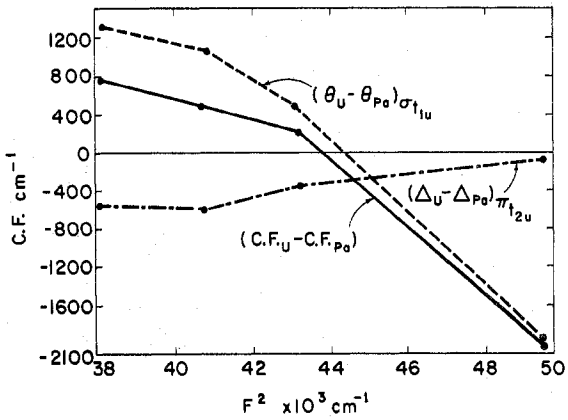

Figure 4. Differences in ligand field parameters for UX_6^{2-} and PaX_6^{2-} vs. F^2 for UX_6^{2-}.

radial extent of the 5f wave function for Pa^{4+}. Judd[19] has pointed out that the observed values of F^2 for the UX_6^{2-} compounds correlate in a roughly linear way with the polarizability of the halide ion, and a qualitative calculation has shown that a nearby polarizable atom or ion will always reduce the effective Coulombic interaction in a second ion.[20] However, these qualitative models suggest larger values for the crystalline field parameters for the Pa complexes, contrary to the observed trends of the chloride, bromide, and iodide compounds.

Another way of interpreting the change in F^2 in this series of complexes is by use of the nephelauxetic effect.[21] We would then expect the electron cloud about the metal ion to expand toward the ligands with the effect to be largest for I^- and smallest for F^-. If we define β' as the ratio F^2(complex)/F^2(free ion) and assume $\beta' = 1$ for UF_6^{2-}, then we find $\beta' = 0.87$ for UCl_6^{2-}, $\beta = 0.82$ for UBr_6^{2-}, and $\beta' = 0.77$ for UI_6^{2-}. This trend follows that found in the d transition series[21] and will explain the changes in F^2. However, it does not explain the large differences between the ligand field parameters of the PaX_6^{2-} and UX_6^{2-} complexes.

Let us assume the crystal field parameters for the PaX_6^{2-} complexes should be valid for the UX_6^{2-} complexes and then consider the differences in the crystal field defined as

$$\Delta CF = CF(U) - CF(Pa) \quad (2)$$

where $CF = \theta + \Delta$. As can be seen from Tables IV and V the crystal (or ligand) field in the series of ligands (I–Br–Cl–F) increases much more rapidly for the PaX_6^{2-} complexes than for the UX_6^{2-} complexes. There will be a point where CF(U) = CF(Pa) ($\Delta CF = 0$) for a hypothetical ligand at a certain bond distance. We call this point "equilibrium" and consider the value found for F^2 at this point as the "correct" value. Figure 4 shows a plot of ΔCF vs. F^2. Qualitatively ΔCF decreases from the iodide to the fluoride as the value of F^2 increases. From this definition of "equilibrium" the value of F^2 appears to be too large for UF_6^{2-} and too small for other members of the UX_6^{2-} series.

This work shows that the parameters obtained in the usual method for analyzing optical data of 4f and 5f series may not have the same meaning for free-ion spectra and solid-state spectra. Our studies suggest the Slater parameter F^2 is strongly affected by the type of ligand in the complex and may absorb some of the effects of the ligand field. Such effects have been predicted by theoretical calculations.[22,23] This is also true to a lesser degree for the spin–orbit coupling constant. If F^2 and ζ are affected by the ligands, then the values found for the ligand field parameters may also not be the "correct" values.

Finally, we wish to point out that our analysis is consistent with the excellent studies of Satten et al.[4-6] The $5f^2$ optical

spectra observed in octahedral symmetry are dominated by the vibronic transitions. Furthermore, the electrostatic, spin–orbit, and crystalline field parameters increase as the ligand changes from I^- to F^-. In the $5f^1$ series the crystalline field and spin–orbit parameters also increase with higher oxidation state on the metal ion. The reported analysis of the optical spectrum of $CsNpF_6$[24] does not fit the above trends. We suggest this discrepancy should be studied further.

Conclusion

We have analyzed the optical spectra of $(NEt_4)_2UF_6$ and $(NEt_4)_2UI_6$. The electrostatic, spin–orbit, and crystal field parameters for the entire UX_6^{2-} (X = F, Cl, Br, I) have been obtained and where applicable compared to corresponding parameters for PaX_6^{2-}. It was noted that the Slater parameter F^2 changes by approximately 20% for the series and the crystal field parameters are dissimilar for the comparable PaX_6^{2-} and UX_6^{2-} complexes.

Acknowledgment. We wish to thank Professor B. R. Judd and Dr. K. Rajnak for illuminating discussions. W. Wagner thanks the Deutscher Akademischer Austauschdienst for its financial support. This work was done with support from the U.S. Energy Research and Development Administration and from NATO Grant 1113.

Registry No. $(Et_4N)_2UF_6$, 42294-80-4; $(Et_4N)_2UI_6$, 56848-06-7; Cs_2UCl_6, 17030-13-6; $(NEt_4)_2UCl_6$, 12081-51-5; $(NEt_4)_2UBr_6$, 12080-72-7.

References and Notes

(1) (a) Lawrence Berkeley Laboratory. (b) Atomic Energy Research Establishment.
(2) (a) N. Edelstein, D. Brown, and B. Whittaker, *Inorg. Chem.*, **13**, 563 (1974); (b) D. Brown, B. Whittaker, and N. Edelstein, *ibid.*, **13**, 1805 (1974).
(3) D. Brown, P. Lidster, B. Whittaker, and N. Edelstein, *Inorg. Chem.*, **15**, 214 (1976).
(4) D. R. Johnston, R. A. Satten, C. L. Schreiber, and E. Y. Wong, *J. Chem. Phys.*, **44**, 3141 (1966).
(5) R. A. Satten, C. L. Schreiber, and E. Y. Wong, *J. Chem. Phys.*, **42**, 162 (1965).
(6) R. A. Satten, D. Young, and D. M. Gruen, *J. Chem. Phys.*, **33**, 1140 (1960).
(7) D. Brown, B. Whittaker, and J. Edwards, Report AERE-R7480, Atomic Energy Research Establishment, 1973 (available from H. M. Stationary Office, London, W.C.1, England).
(8) B. R. Judd, "Operator Techniques in Atomic Spectroscopy", McGraw-Hill, New York, N.Y., 1963.
(9) B. G. Wybourne, "Spectroscopic Properties of Rare Earths", Interscience, New York, N.Y., 1965.
(10) In our calculations we have used as the electrostatic interaction parameters the Slater radial integrals F^k (k = 2, 4, 6). These integrals have been redefined by Condon and Shortley[11] as $F_2 = F^2/225$, $F_4 = F^4/1089$, and $F_6 = F^6/7361.64$, for an f^n configuration.
(11) E. U. Condon and G. H. Shortley, "The Theory of Atomic Spectra", Cambridge University Press, Cambridge, 1935.
(12) K. Rajnak, *Phys. Rev. A*, **14**, 1979 (1976).
(13) W. von der Ohe, *J. Chem. Phys.*, **62**, 3933 (1975).
(14) J. Shamir and A. Silberstein, *J. Inorg. Nucl. Chem.*, **37**, 1173 (1975).
(15) S. L. Chodos and R. A. Satten, *J. Chem. Phys.*, **62**, 2411 (1975).
(16) D. Brown, B. Whittaker, and P. E. Lidster, Report AERE-R8035, Atomic Energy Research Establishment, 1975 (available from H. M. Stationary Office, London, W.C.1, England).
(17) J. L. Ryan, J. M. Cleveland, and G. H. Bryan, *Inorg. Chem.*, **13**, 214 (1974).
(18) W. T. Carnall, private communication.
(19) B. R. Judd, private communication.
(20) B. R. Judd, *Math. Proc. Cambridge Philos. Soc.*, in press.
(21) C. E. Schäffer and C. K. Jørgensen, *J. Inorg. Nucl. Chem.*, **8**, 143 (1958).
(22) K. Rajnak and B. G. Wybourne, *J. Chem. Phys.*, **41**, 565 (1964).
(23) S. S. Bishton and D. J. Newman, *J. Phys. C*, **3**, 1753 (1970).
(24) L. P. Varga, J. D. Brown, M. J. Reisfeld, and R. D. Cowan, *J. Chem. Phys.*, **52**, 4233 (1970).

Contribution from the Department of Chemistry, University of Rajasthan, Jaipur, India

Kinetics and Mechanism of the Oxidation of Arsenic(III) by Hexacyanoferrate(III) in Alkaline Medium

DEVENDRA MOHAN, DINESH GUPTA, and Y. K. GUPTA*

Received June 3, 1976 AIC60443L

Kinetics of the reaction between hexacyanoferrate(III) and arsenic(III) in alkaline medium has been reinvestigated to establish As^{III} and OH^- dependences. The rate depends on the ratio $[OH^-]/[As^{III}]$. The rate law for $[OH^-]/[As^{III}] > 1$ is $-d[Fe(CN)_6^{3-}]/dt = [Fe(CN)_6^{3-}][As^{III}](k_1K_1[OH^-] + k_2K_1K_2[OH^-]^2 + k_3K_1K_2K_3[OH^-]^3)/(1 + K_1[OH^-] + K_1K_2[OH^-]^2 + K_1K_2K_3[OH^-]^3)$. k_1, k_2, and k_3K_3 were found to be $(10 \pm 0.9) \times 10^{-3}$ M^{-1} s^{-1}, 0.35 ± 0.02 M^{-2} s^{-1}, and 13 ± 0.2 M^{-3} s^{-1}, respectively, at 45 °C and I = 2.0 M. K_1, K_2, and K_3 are the equilibrium constants for the formation of $H_2AsO_3^-$, $HAsO_3^{2-}$, and AsO_3^{3-} from H_3AsO_3 and OH^-. E_a and ΔS^* associated with k_1, k_2, and k_3K_3 were found to be 11.8 ± 0.5, 6.4 ± 0.7, and 3.75 ± 0.46 kcal mol^{-1} and -32 ± 2, -43 ± 3, and -42 ± 3 cal mol^{-1} deg^{-1}, respectively.

Introduction

Krishna and Singh[1] and Mushran and co-workers[2] have investigated the kinetics of the oxidation of arsenic(III) by hexacyanoferrate(III) ion in alkaline solutions. The effect of hexacyanoferrate(III) ion has been variously reported. A limited range of concentrations had been employed to study the arsenite and hydroxide ion dependences. The various equilibria involving arsenic(III) and OH^-, as reported by Mushran and co-workers,[2] clearly indicate that the arsenite and hydroxide ion dependences would depend on their ratios but they did not give quantitative treatment. These were some of the points which prompted us to reinvestigate the kinetics of this reaction. About a 1000-fold variation in the concentration of As^{III} and about 500-fold variation in the concentration of NaOH have enabled us to characterize the various rate constants. The overall reaction is represented by

$$As^{III} + 2Fe(CN)_6^{3-} \rightarrow As^{V} + 2Fe(CN)_6^{4-}$$

Experimental Section

The stock solution of 0.2 N arsenious acid was prepared by dissolving the requisite amount of arsenic trioxide, sufficient to give a little more than 0.20 N acid, in boiling water. After cooling, it was filtered and standardized against a standard permanganate solution. All other reagents used were BDH AnalaR. Doubly distilled water was used throughout (the second distillation being from the permanganate).

Reactions were carried out in a thermostated water bath at 45 ± 0.1 °C unless mentioned otherwise. Measured quantities of As^{III} and sodium hydroxide solutions were mixed and kept in the water bath